physica status solidi

pss

www.pss-journals.com

reprint

WILEY-VCH

Phys. Status Solidi C **10**, No. 2, 160–164 (2013) / **DOI** 10.1002/pssc.201200474

physica status solidi c
www.pss-c.com
current topics in solid state physics

First-principles modeling of the *H* color centers in MgF_2 crystals

Alma Dauletbekova[*,1], Fatima Abuova[,1], Abdirash Akilbekov[1], Eugene Kotomin[2], and Sergey Piskunov[2]**

[1] L.N. Gumilyov Eurasian National University, 5 Munaitpassov str., 010008 Astana, the Republic of Kazakhstan
[2] Institute of Solid State Physics, University of Latvia, 1063 Riga, Latvia

Received 12 July 2012, revised 10 November 2012, accepted 15 November 2012
Published online 19 December 2012

Keywords MgF_2, point defects, *H*-centers, atomic and electronic structure, first-principles calculations

* Corresponding author: e-mail alma_dauletbek@mail.ru, Phone: +7 7172 342 013, Fax: +7 7172 353 806
** e-mail fatika_82@mail.ru, Phone: +7 7172 342 013, Fax: +7 7172 353 806

MgF_2 with a rutile structure is important wide-gap optical material with numerous applications. We present and discuss the results of calculations for basic hole defects – interstitial F atoms (called also the colour *H* centers). This study is based on the large scale *ab initio* DFT calculations using hybrid B3PW exchange-correlation functional as implemented into CRYSTAL computer code. The electronic structure, atomic geometry, charge density distribution are calculated and compared with similar defects in CaF_2 fluorite. It is shown that the *H* centers oriented nearly parallel to the (110) axis are energetically more favourable than those oriented along the (001) axis, in agreement with experiment.

1 Introduction Optical devices made of magnesium fluoride (MgF_2) are transparent over an extremely wide range of photon energies, from vacuum ultraviolet to infrared. It is also radiation-resistant material, the energy required to form a stable primary radiation defect known as the *F* center (fluorine vacancy with trapped electron) between 5K and room temperature is much higher than in other alkali halides [1]. To our opinion, this could be related to efficient diffusion-controlled recombination of the primary radiation defects in MgF_2 - the complementary F and H centers (interstitial fluorine ions); most of highly moblile H centers meet F centers during secondary reactions whereas only their small fraction are aggregated and thus avoid recombination.

These two factors make MgF_2 an important material for space telescopes and similar applications. However, it is essential for materials scientists to understand at the atomistic level reasons of MgF_2 high radiation stability. Despite several *ab initio* calculations of basic MgF_2 properties (both bulk [2, 3] and surfaces [4, 5]), we are not familiar with studies of this material with defects at the *ab initio* level (unlike other fluorites, CaF_2, SrF_2 and BaF_2 [6-8]). In this paper, we present results of *ab initio* calculations of the *H* centers in the MgF_2 bulk of crystals.

2 Computational method MgF_2 (rutile) has a tetragonal $P4_2/mnm$ structure with two formula units in the unit cell. As in previous calculations on the MgF_2 bulk and (001) surface [4, 5], we used the CRYSTAL computer code [9] using localized, Gaussian-type basis sets. Our spin-polarized calculations were performed using the DFT-HF hybrid exchange-correlation B3PW functional [10] which gives better agreement of calculated and experimental MgF_2 optical gap than when applying other functional: 9.5 eV (B3PW) *vs.* 19.65 eV (HF), 6.9 eV (GGA-PBE), (*cf.* with the experimental value of 12.5 eV, see Ref. [4]). The reciprocal space integration was performed by sampling the Brillouin zone with a 5 × 5 × 5 Pack-Monkhorst mesh [11]. To achieve high accuracy, large enough tolerances of 7, 8, 7, 7, and 14 were chosen for the Coulomb overlap, Coulomb penetration, exchange overlap, first exchange pseudo-overlap, and second exchange pseudo-overlap, respectively [8]. In our calculations for MgF_2 we applied the basis set developed by Catti et al. for the F atom [12] and by McCarthy and Harrison [13] for the Mg atom. The effective atomic charges were calculated using the Mulliken population analysis [14].

To simulate the *H* centers, we used a 2 × 2 × 2 times expanded unit cell (3% defect concentration) containing 48 atoms. An interstitial F atom was then introduced therein and its chemical bonding with regular F ions was studied. It is well known that typical hole defects in alkali halides and fluorites are so-called split interstitials (dumbbells), *e.g.* F_2^- ions in the singlet state (one unpaired electron) [15]. These defects are complementary to the *F* centers (fluorine vacancy). As a result of calculations, we obtained the relaxed lattice geometry, effective atomic charges and interatomic bond populations, the band structure, density of states (DOS) and defect formation energies.

3 Main results We found two possible orientations of the *H* centers, with the interatomic bonds oriented along the (001) and (110) directions (Fig. 1a, b, respectively).

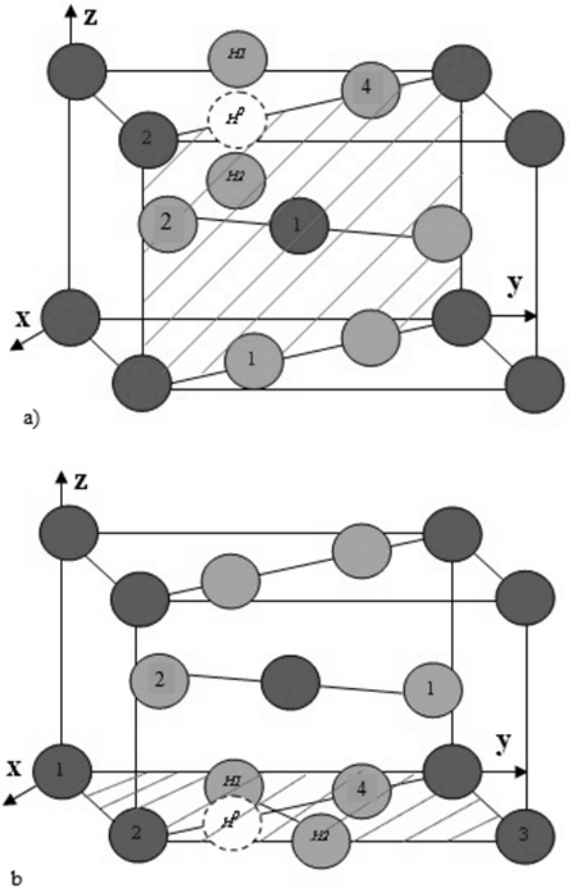

Figure 1 Schematic view of the (001) and (110) oriented *H* centers (a and b, respectively). H^0 is a position of a regular F ion before defect formation. Light and dark circles are F and Mg ions, respectively

The latter configuration is lower in energy (by 0.37 eV) than the former one, in agreement with the experiment [16]. The equilibrium interatomic distances in the (110) and (001) *H* centers are 1.96 Å and 1.82 Å, respectively. (Notice that the distance in the free F_2^- molecule is 1.98 Å, that is both molecular ions are compressed in a crystal, more in the (001) direction.)

The effective charges of the F and Mg ions in a perfect MgF_2 are -0.9 e and 1.80 e, respectively [4, 5], which indicates a high ionicity of this material. When additional F49 atom is introduced into the interstitial position of the 48-atom supercell, in the (110) direction (Fig. 2), it shares the electron density almost equally with two nearest F ions (the effective charges are -0.59 e (F-49) *vs*. -0.68 e (*H1* and *H2*), respectively. After forming a chemical bond with one of these F ions, the effective charges of the two atoms of the *H* center along the (100) direction become -0.46 e each whereas the total spin on these fluorines is 0.92 μ_B. That is, this defect is very close to the classical *H* center model [15]. The effective atomic charges are presented in Tables 1 and 2. The above-discussed is well illustrated by the electron density maps in Fig. 3a, b.

Note that transformation of the interstitial fluorine atom into the *H* center happens spontaneously and is accompanied with the energy gain, in agreement with experiment – and in contrast to the plane wave DFT calculations in CaF_2 [8] where interstitial atom is lower in energy. This shown an advantage of the calculations with hybrid exchange-correlation functionals and atomic basis sets

Table 1 Effective charges (e) of *H* centers oriented along the [001] axis, ΔQ (e) are charge deviations from perfect crystal.

Shells	Q	ΔQ	Spin
H2	-0.460	0.438	0.473
H1	-0.459	0.439	0.475
Mg1	1.912	-0.115	0
Mg2	1.923	-0.126	-0.001
Mg 3	1.912	-0.115	0
F1	-0.963	-0.065	0.044
F2	-0.965	-0.067	0
F3	-0.963	-0.065	0.002
F4	-0.966	-0.068	-0.001

Table 2 The same as Table 1 along the [110] axis.

Shells	Q	ΔQ	Spin
H2	-0.312	0.586	0.619
H1	-0.768	0.13	0.234
Mg1	1.92	-0.123	0
Mg2	1.924	-0.127	0
Mg3	1.923	-0.126	0
F1	-0.970	-0.072	0.001
F2	-0.964	-0.066	0.002
F3	-0.870	0.028	0.135
F4	-0.950	-0.052	0

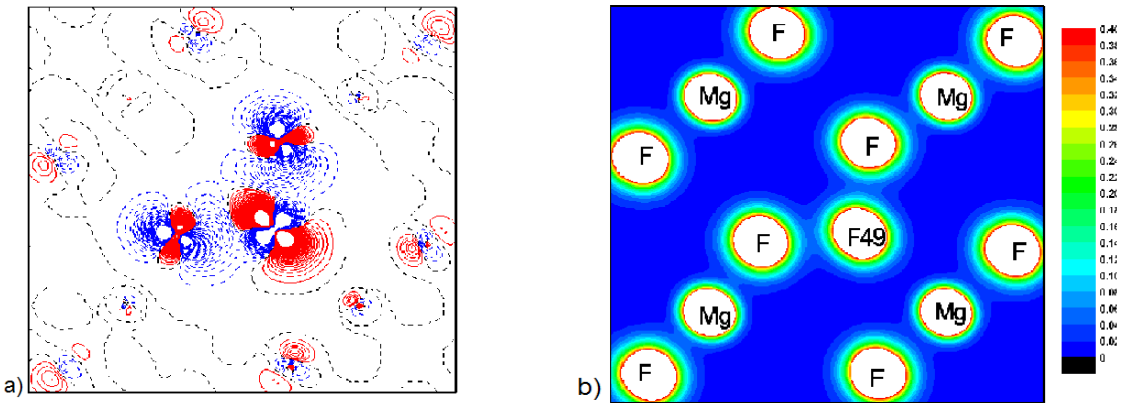

Figure 2 The total (b) and difference (a) electronic density maps for the additional F atom (F-49) incorporated into the 48-atom supercell of the perfect MgF_2. The full and dashed colours indicate electron density deficiency and excess, respectively. The density range is from 0 to 0.4 *e*/Bohr^3 with increment of 0.02 *e*/Bohr^3

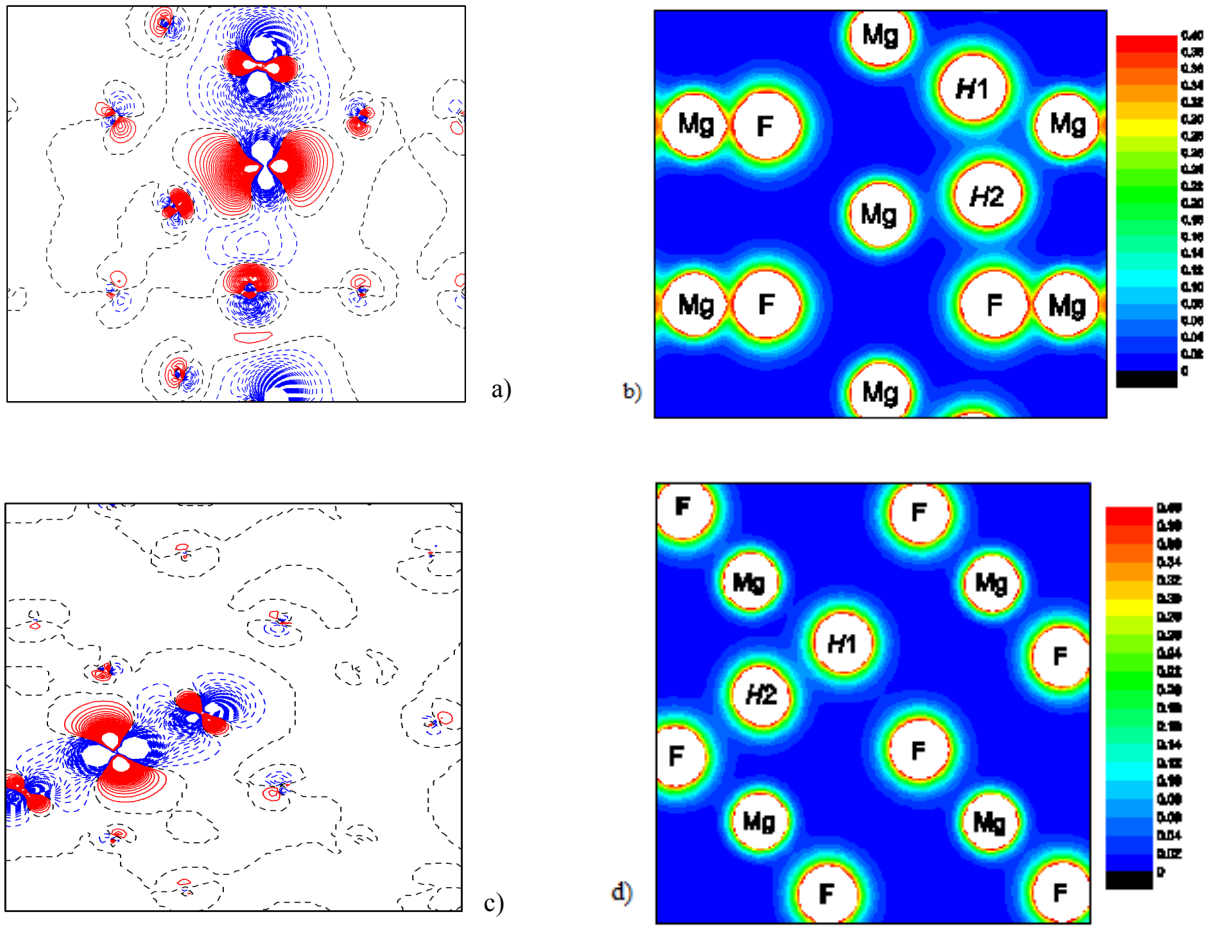

Figure 3 The difference and total electron density redistribution around the *H* centers in the (001) (a,b) and the (110) (c,d) planes (see Fig. 1). The density range is from 0 to 0.4 *e*/Bohr^3 with increment of 0.02 *e*/Bohr^3

Table 3 Atomic displacements around *H* center along the (001) direction. Atomic labels are shown in Fig. 1.

	Displacements					
	Δ x (Å)	Δ x/a %	Δ y (Å)	Δ y/b %	Δ z (Å)	Δ z/c %
H1	-0.303	6.51	-0.303	6.51	0.930	29.62
H2	-0.137	2.94	-0.137	2.94	0.083	2.64
Mg1	0.148	3.18	0.148	3.18	0.084	2.68
Mg 2	0.144	3.09	0.144	3.09	0.019	0.60
Mg 3	0.148	3.18	0.148	3.18	0.039	1.24
F1	-0.56	12.03	-0.560	12.03	0.023	0.73
F2	0.436	9.36	0.571	12.30	0.008	0.27
F3	-0.32	6.88	-0.320	6.88	0.009	0.29
F4	-0.499	10.72	-0,499	10.72	0.020	0.63

Table 4 The same as Table 3 for the (110) direction.

	Displacements					
	Δ x (Å)	Δ x/a %	Δ y (Å)	Δ y/b %	Δ z (Å)	Δ z/c %
H1	0.830	17.8	-0.253	5.44	0	0
H2	0.248	5.33	0.411	8.83	0	0
Mg1	0.0422	0.9	0.0133	0.29	0	0
Mg2	-0.017	0.36	-0.016	0.34	0	0
Mg3	-0.066	1.42	-0.016	0.34	0	0
F1	0.375	8.06	0.578	12.4	0.065	2.07
F2	-0.588	12.63	-0.504	10.8	0.029	0.9
F3	-0.641	13.77	-0.347	7.5	0	0
F4	0.480	10.31	-0.510	10.9	0	0

Table 5 Coordinates of atoms around *H* center along (001) axis.

Neighbors of *H*-center	Coordinates		
	x (Å)	y(Å)	z(Å)
H^0	-1.42	-1.42	1.57
H1	-1.12	-1.12	2.5
H2	-1.12	-1.12	0.68
Mg 1	0.15	0.15	-0.08
Mg 2	-2.47	-2.47	1.59
Mg 3	0.15	0.15	-3.1
F 1	-0.85	-0.85	-1.59
F 2	-1.34	1.49	-0.01
F 3	3.43	-3.43	-0.01
F 4	0.92	0.92	1.59

Table 6 The same as Table 5 along the (110) axis.

Neighbors of *H*-center	Coordinates		
	x (Å)	y(Å)	z(Å)
H^0	3.75	0.91	0
H1	2.92	1.16	0
H2	4.56	2.23	0
Mg 1	-0.04	-0.01	0
Mg 2	-4.64	-0.01	0
Mg 3	4.59	4.64	0
F 1	3.61	3.81	-1.64
F 2	0.83	0.92	-1.6
F 3	-3.1	3.4	0
F 4	1.4	3.24	0

When the *H* center is oriented along the (110) axis (Fig. 3c, d), atomic charges are distributed strongly asymmetrically (Table 2): -0.31 e (*H1*) and -0.77 e (*H2*). This observation is in agreement with EPR experiments [17], where the atomic charge distribution was estimated as 0.4 e – 0.6 e. As mentioned in this paper, this asymmetry could be a reason for increased annealing temperature of these defects. The spins on these two atoms are also inequal: $0.62\mu_B$ and $0.23\mu_B$, respectively.

Atomic displacements (absolute values and relative) produced by the *H* center formation are presented in Table 3 and 4, for the (001) and (110) defect orientations, respectively, whereas absolute coordinates of ions are given in Tables 5 and 6, respectively. Note that in the (001) center the displacements of *H1* and *H2* ions are strongly anisotropic: the former ion is strongly displaced from a regular lattice site (H^0), whereas the latter ion is close to the lattice site. This is a reason of discussed asymmetry in the effective charges for *H1* and *H2* ions. Note also that the F ions are displaced in general larger than the Mg ions.

We could compare our calculations with a similar study of the *H* center in CaF_2 showing the fluorite structure. The B3PW hybrid functional calculations show [7] that the most stable defect orientation is along the (111) axis which is by 0.83 eV lower in energy rather the (100) one, in agreement with the experiment. The hole density distribution is asymmetric (as in our case), with F ion charges -0.659 e and -0.287 e, with nearest Ca ion displacements ca. 1% of the lattice constant. In contrast, the charge distribution in the less stable (100) H center is symmetric, also similarly to our calculations for the (001) center in MgF_2.

4 Conclusions Our *ab initio* DFT calculations confirm the experimental conclusion [16,17] that the (110) oriented *H* center is energetically more favourable in MgF_2 than the (001) one. Our calculations predict the difference in energies to be 0.37 eV and slight deviation of the bond orientation from the (110) axis. The (001) oriented *H* centers are symmetrical, with similar effective charges and spins on both atoms, unlike strongly asymmetric (110) *H*

centers. In both cases, formation of the chemical bonds of the interstitial F atom with a regular F ion is energetically favourable. Calculations of complementary F centers and radiation-induced *F*-*H* pairs of Frenkel defects are in progress.

Acknowledgements Authors are indebted to Prof. V. N. Lisitsyn for many stimulating discussions.

References

[1] R. F. Blunt and M. I. Cohen, Phys. Rev. **153**, 1031 (1967). M. R. Buckton and D. Pooley, J. Phys. C **5**, 1553 (1972).
[2] M. Catti, A. Pavese, R. Dovesi, C. Roetti, and M. Causa, Phys. Rev. B **44**, 3509 (1991).
[3] K. R. Babu, Ch. B. Lingam, S. Auluck, S. P. Tewari, and G. Vaitheeswaran, J. Solid State Chem. **184**, 343 (2011).
[4] A. F. Vassilyeva, R. I. Eglitis, E. A. Kotomin, and A. K. Dauletbekova, Physica B **405**, 2125 (2010).
[5] A. F. Vassilyeva, R. I. Eglitis, E. A. Kotomin, and A. K. Dauletbekova, Cent. Eur. J. Phys. **9**, 515 (2011).
[6] H. Shi, R. I. Eglitis, and G. Borstel, Phys. Rev. B **72**, 045109 (2005).
[7] H. Shi, R. I. Eglitis, and G. Borstel, J. Phys.: Condens. Matter **18**, 8367 (2006).
[8] A. S. Foster, T. Trevathan, and A. L. Shluger, Phys. Rev. B **80**, 115421 (2009).
[9] V. R. Saunders, R. Dovesi, C. Roetti, M. Causa, N. M. Harrison, R. Orlando, and C. M. Zicovich-Wilson, Crystal User Manual (University of Torino, Italy, 2006).
[10] A. D. Becke, J. Chem. Phys. **98**, 5648 (1993).
[11] H. J. Monkhorst and J. D. Pack, Phys. Rev. B **13**, 5188 (1976).
[12] M. Catti, R. Dovesi, A. Pavese, and V. R. Saunders, J. Phys.: Condens. Matter **3**, 4151 (1991).
[13] M. I. McCarthy and N. M. Harrison, Phys. Rev. B **49**, 8574 (1994).
[14] C. R. A. Catlow and A. M. Stoneham, J. Phys. C **16**, 4321 (1983).
[15] A. M. Stoneham, Theory of Defects in Solids (Cambridge Univ. Press, 1975).
[16] C. D. Norman and L. E. Halliburton, Phys. Rev. B **15**, 5883 (1977).
[17] Y. Ueda, J. Phys. Soc. Jpn. **41**, 1255 (1976).

